SLAC-PUB-764
June 1970
(TH) and (EXP)

ANALYSIS OF DIFFERENTIAL AND TOTAL CROSS SECTION DATA FOR HIGH ENERGY pp AND $p\bar{p}$ INTERACTIONS

Wolfgang Drechsler* and Roberto Suaya**

Stanford Linear Accelerator Center
Stanford University, Stanford, California 94305

ABSTRACT

An analysis of pp and $p\bar{p}$ data in terms of a K-matrix model for the Pomeranchuk exchange and the absorptive corrected P' and ω Regge pole contributions is presented. The model provides a quantitative understanding of high energy pp and $p\bar{p}$ total cross section measurements and the measured ratio of the real to imaginary part of the pp elastic forward scattering amplitude. The structure observed in $(d\sigma/dt)_{p\bar{p}}$ around $t=-0.8$ GeV^2, in $(d\sigma/dt)_{pp}$ at $t=-1.2$ GeV^2, the shrinkage patterns in both differential cross sections, as well as the crossover phenomenon are explained in the framework of this model.

(Submitted to Phys. Rev.)

* Work supported in part by the U. S. Atomic Energy Commission and the Max Kade Foundation.

** Fellow from the University of Buenos Aires.

In a recent publication[1] a K-matrix model for the Pomeranchuk exchange contribution to high energy elastic scattering and diffraction dissociation processes has been proposed which is confronted in this letter with differential and total cross section measurements for high energy pp and $p\bar{p}$ collisions. The main feature of the proposed model for Pomeranchuk exchange is that the vacuum exchange contribution is thought to originate from multiple exchange of various lower lying trajectories, having an intercept $\alpha(0)=0.5$ and a slope $\alpha'=1\,\mathrm{GeV}^{-2}$, accompanied by the formation of a sequence of intermediate excited states (resonances) of the colliding particles. The model at the present stage does not account for spin flip contributions. It can be regarded as a unitarized relativistic multiple scattering model for spinless incoming and outgoing particles. In terms of j-plane singularities the proposed interpretation of the vacuum exchange contribution corresponds to a superposition of cuts in the complex angular momentum plane. However, the number of parameters describing the Pomeranchuk contribution is two as in the conventional Pomeranchuk pole model.

The amplitudes for elastic scattering and diffraction dissociation processes are written down in the impact parameters language[2] neglecting spin and isospin, and are made unitary by a multichannel K-matrix parameterization assuming an effective two-particle description for the inelastic states in the unitarity relations. The attractive features of this model for the Pomeranchuk contribution are that it predicts (1) logarithmic shrinkage of diffraction peaks up to very high energies corresponding to an effective Pomeranchuk pole of slope $\alpha'_{P,\mathrm{eff}}=\frac{\alpha'}{2}$ in agreement with the recent measurements from Serpukhov,[3] and (2) a logarithmic approach to asymptotic conditions for total cross sections similar to other multiple scattering approaches to the vacuum exchange contribution.[4] Furthermore, a natural explanation for the crossover phenomenon is provided in terms of absorptive corrections to the input Regge Born terms. We shall show below that the model is, moreover,

able to reproduce the structure in the pp differential cross section at $t \approx -1.2$ GeV^2 and in the $p\bar{p}$ differential cross section between $t=-0.6$ and -0.9 GeV^2. We, however, find that the present spinless treatment is unable to account for $(d\sigma/dt)_{pp}$ beyond $t=-2$ GeV^2. We are inclined to attribute this observation to nonnegligible spin flip contributions being present at momentum transfer larger than $|t|=2$ GeV^2 where the pp differential cross section at $p_{lab}=19.2$ GeV/c has gone down by nearly five orders of magnitude compared to the value at $t=0$.

Before we proceed, we collect the relevant formulae partly derived in Ref. 1. In the equations written below the upper sign refers to pp scattering whereas the lower sign refers to $p\bar{p}$ scattering. Besides the diffractive contribution we take only P' and ω exchange in the t-channel into account. Possible small $\rho, A2, \pi$ or B contributions are neglected.[5]

The differential cross section and the optical theorem read

$$\frac{d\sigma}{dt} = \frac{1}{4\pi q^2 s} |f(s,t)|^2 \tag{1}$$

$$\text{Im } f(s,t=0) = 1/2\ q\sqrt{s}\ \sigma_{tot}(s) \tag{2}$$

with

$$f(s,t) = 2\pi s \int_0^\infty bdb\ \eta(b,s)\ J_0(b\sqrt{-t}) \tag{3}$$

where

$$\eta(b,s) = \frac{iC(b,s) - D(b,s)}{1 + C(b,s) + iD(b,s)} + \left[N^{P'}(b,s) \pm N^{\omega}(b,s)\right] \cdot \frac{1 - C(b,s) - 2i\,D(b,s)}{\left[1 + C(b,s) + iD(b,s)\right]^2} \tag{4}$$

Here s is the total energy squared and $q = \frac{1}{2}\sqrt{s - 4m_P^2}$ is the relative momentum with m_P denoting the proton mass. C(b,s) and D(b,s) in Eq. (4) are given by

$$C(b,s) = Q(s)\ e^{-b^2/2\rho}\ ; \qquad D(b,s) = R(s)\ e^{-3b^2/4\rho} \tag{5}$$

where $\rho = \alpha' \log s/s_0$ and [6]

$$Q(s) = \frac{\sigma_{tot}(\infty)}{8\pi\,\alpha' \log \frac{s}{s_0}}\ ; \qquad R(s) = \frac{\tau}{8\pi\,\alpha' \log \frac{s}{s_0}} \tag{6}$$

The quantities $N^{P',\omega}(b,s)$ represent the Fourier Bessel transforms of the single Regge exchange terms, $g^{P',\omega}(s,t)$, for P' and ω exchange, respectively, which are defined in Eq. (13) below. In Eq. (6) α' is the slope of the particle trajectories which generate the Pomeranchuk contribution via multiple exchange and resonance excitation in the above described way. In the derivation of Eq. (4) it was assumed in Ref. 1 that s is large and that the real part of the diffractive contribution, measured by D(b,s), is small compared to the imaginary part determined by C(b,s). Separating the real and imaginary parts in Eq. (4) and neglecting terms of order $\left(\tau/\sigma_{tot}(\infty)\right)^2$ one obtains, besides a vacuum contribution to $\mathrm{Im}\,\eta(b,s)$ and $\mathrm{Re}\,\eta(b,s)$, an absorptive correction to the input Regge pole terms at impact parameter b and total energy squared s determined by the functions A(b,s) and B(b,s) (compare the second term in Eqs. (8) and (11) below) which are given by:

$$A(b,s) = 4\,\frac{R(s)\,e^{-3b^2/4\rho}}{\left[1+Q(s)\,e^{-b^2/2\rho}\right]^3} \quad ; \qquad B(b,s) = \frac{1-Q(s)\,e^{-b^2/2\rho}}{\left[1+Q(s)\,e^{-b^2/2\rho}\right]^2} \tag{7}$$

We finally write down the expression for the total cross sections and the ratio of the real to imaginary part of the elastic forward scattering amplitudes in the K-matrix model for Pomeranchuk exchange:

$$\sigma_{tot}(s) = \sigma^{P}_{tot}(s) + \frac{4\pi\sqrt{s}}{q}\left[\int_0^\infty bdb\left\{\mathrm{Im}\left[N^{P'}(b,s) \pm N^{\omega}(b,s)\right] B(b,s) - \mathrm{Re}\left[N^{P'}(b,s) \pm N^{\omega}(b,s)\right] A(b,s)\right\}\right] \tag{8}$$

Here the Pomeranchuk contribution to the total cross section is given by

$$\sigma^{P}_{tot}(s) = \frac{4\pi\alpha'\sqrt{s}}{q}\,\log\frac{s}{s_0}\,\log\left[1+\frac{\sigma_{tot}(\infty)}{8\pi\alpha'\log\frac{s}{s_0}}\right] \tag{9}$$

For extremely high energies the right-hand side of Eq. (9) approaches the constant value $\sigma_{tot}(\infty)$, which was the reason for having introduced this constant in Eq. (6).

The value of τ is related in a simple manner to the ratio of the real to imaginary part of the elastic forward scattering amplitude for both pp and $p\bar{p}$ at infinite energies according to

$$\lim_{s \to \infty} \frac{\text{Re } f(s,t=0)}{\text{Im } f(s,t=0)} = \xi(\infty) = -\frac{2}{3}\frac{\tau}{\sigma_{tot}(\infty)} \tag{10}$$

At nonasymptotic s one finds:

$$\xi(s) = \frac{\text{Re } f(s,t=0)}{\text{Im } f(s,t=0)} = \tilde{\xi}(s) + \frac{4\pi\sqrt{s}}{q\sigma_{tot}(s)}\left[\int_0^\infty bdb \left\{\text{Re}\left[N^{P'}(b,s) \pm N^{\omega}(b,s)\right] B(b,s) + \text{Im}\left[N^{P'}(b,s) \pm N^{\omega}(b,s)\right] A(b,s)\right\}\right] \tag{11}$$

where $\sigma_{tot}(s)$ is given by Eq. (8) and $\tilde{\xi}(s)$ is given by

$$\tilde{\xi}(s) = -\frac{2}{3}\frac{\tau}{\sigma_{tot}(s)}\sqrt{\frac{s}{s-4m_p^2}}\int_0^1 \frac{dx}{\left[1+Q(s)\,x^{2/3}\right]^2} \tag{12}$$

which, for $s \to \infty$, tends to the constant limit (10).

Let us now turn to the numerical analysis. We first determined a fit to the data for $\sigma_{tot}^{pp}(s)$, $\sigma_{tot}^{p\bar{p}}(s)$, and $\sigma^{pp}(s)$.[7] As input Regge pole terms we used the following P' and ω contributions

$$g^{P'}(s,t) = -\frac{1}{2}\left(1+e^{-i\pi\alpha_{P'}(t)}\right)\beta_{P'}\left(\frac{s}{s_0}\right)^{\alpha_{P'}(t)};$$
$$g^{\omega}(s,t) = -\frac{1}{2}\left(1-e^{-i\pi\alpha_{\omega}(t)}\right)\beta_{\omega}\left(\frac{s}{s_0}\right)^{\alpha_{\omega}(t)} \tag{13}$$

where $\beta_{P'}$ and β_{ω} are supposed to be constants and $\alpha_{P',\omega}(t) = \alpha_{P',\omega}(0) + t$. Notice that in order to allow a Fourier Bessel transformation to be made we have assumed a certain ghost killing mechanism being operative to remove the poles of the factor $\frac{1}{\sin \pi\alpha(t)}$ appearing in the usual Regge pole expressions. In Ref. 1 we introduced a weaker ghost eliminating mechanism which was called minimal ghost killing there, being different for positive and negative signature trajectories.

To fit the total cross section data and in particular the relatively weak s-dependence of $\sigma_{tot}^{pp}(s)$, which comes about through a cancellation of the P' and ω contributions, it turned out, however, that the minimal ghost killing mechanism is not tenable and Eqs. (13) had to be used as input.

The fit obtained, using the program MINFUN of Berkeley-SLAC had a χ^2 of 24.7 for 41 data points and 7 parameters, is shown by the curves labelled I in Figs. 1a and 1b. The energy dependence of the total cross sections is well represented. The resulting values for the parameters are:

$$\text{(I)} \quad \begin{aligned} &\sigma_{tot}(\infty) = 119.8 \text{ GeV}^{-2}; \quad \alpha_{P'}(0) = 0.58 \; ; \quad \beta_{P'} = 79.8 \\ &\tau = -20.4 \text{ GeV}^{-2}; \quad \alpha_{\omega}(0) = 0.42 \; ; \quad \beta_{\omega} = 54.3 \; ; \quad s_0 = 0.421 \end{aligned}$$

The curve labelled P in Fig. 1a corresponds to the Pomeranchuk contribution alone. The above value of $\sigma_{tot}(\infty)$ of 46 mb coincides with the result obtained by Barger and Phillips[8] in fitting their cut model to essentially the same data. Observe, however, that these authors introduce in addition to a Pomeranchuk pole a cut contribution which turns out to require a negative coefficient. In our K-matrix approach such a contribution is automatically contained in the Pomeranchuk term. Furthermore, the real part of the vacuum contribution comes out to be negative and small compared to the imaginary part.[9] The ratio $\text{Re}\, f(s,t=0)/\text{Im}\, f(s,t=0)$ for pp is predicted to change sign at about p_{lab}=60 GeV/c. The asymptotic value of $\xi^{pp}(s)$ and $\xi^{p\bar{p}}(s)$ is $\xi(\infty) = +0.11$.

We now used the Solution I to make a prediction for the pp and $p\bar{p}$ differential cross sections and compared it with the pp data at 10.94, 12.0 and 12.4 GeV/c and the $p\bar{p}$ data at 11.8 and 12.0 GeV/c.[10] The model provided a reasonable prediction for t-values in the range $0 \leq |t| \leq 0.6$ GeV^2 although the theoretical values corresponding to the above parameters come out in the low t range in both cross sections systematically somewhat bigger than the experimental values. The crossover of the predicted curves occurs at $t = -0.20$ GeV^2, i.e., exactly where the experimental crossover of $(d\sigma/dt)_{pp}$ and $(d\sigma/dt)_{p\bar{p}}$ appears at this energy. This result differs from the one

obtained in Ref. 1 (and also in Ref. 7) due to the different ghost killing mechanism involved as required by the fit to the total cross section data and the real to imaginary part of the forward scattering amplitude. The striking feature of the calculation for $(d\sigma/dt)_{p\bar{p}}$ with the parameters I is the dip bump structure which appears between $-t=(0.6-0.9)$ GeV^2. The structure is similar to the one shown in Fig. 3, Curve I, corresponding to $p_{lab}=16.0$ GeV/c, showing that this type of interference phenomenon producing structure in differential cross sections persists to rather large energies.

To determine the energy dependence of the diffraction peaks in this model we repeated the described comparison at somewhat higher energies, i.e., at $p_{lab}=16.0$ GeV/c for $p\bar{p}$ and at $p_{lab}=19.2$ GeV/c for pp.[11] The agreement in the interval $0\leq|t|\leq 0.6$ GeV^2 was slightly better although the prediction lies still systematically above the experimental points. The general structure of the theoretical curves corresponding to Solution I is the same as at the lower energies and is shown by the curves labelled I in Figs. 2 and 3. In going from 12 to 16 GeV/c, the model predicted a small but noticeable amount of antishrinkage for $(d\sigma/dt)_{p\bar{p}}$, whereas no appreciable shrinkage in the pp case could be detected between 12 and 19.2 GeV/c.

We now made a search for a combined solution for $(d\sigma/dt)_{pp}$ at 19.2 GeV/c; $(d\sigma/dt)_{p\bar{p}}$ at 16 GeV/c, $\sigma_{tot}^{pp}(s)$, $\sigma_{tot}^{p\bar{p}}(s)$ and $\xi^{pp}(s)$. The main problem consisted in estimating how far out in t our spinless model could be used to represent the data. After some numerical tests we finally decided to limit the t-range and to include only those experimental points for elastic pp scattering with $|t|\leq 2.0$ GeV^2. The obtained fits are shown by the curves labelled II in Figs. 1-3. The values for the parameters for this combined fit are

$$\text{(II)}\qquad \begin{aligned} &\sigma_{tot}(\infty) = 118.6; \quad \alpha_{P'}(0) = 0.38 \; ; \quad \beta_{P'} = 64.9 \\ &\tau = -7.64; \quad \alpha_{\omega}(0) = 0.34 \; ; \quad \beta_{\omega} = 53.1 \; ; \quad s_0 = 0.082 \end{aligned}$$

$\sigma_{tot}(\infty)$ is essentially unchanged compared to Solution I; τ is considerably smaller and we loose the good description of $\xi^{pp}(s)$ obtained before. We show by the curves labelled P in Figs. 2 and 3 the Pomeranchuk contribution to the differential cross

sections. To first order in τ these curves are independent on τ.[12] As is clear from Fig. 2 the shoulder of the pp differential cross section at $t=-1.2$ GeV^2 comes out very nicely in this model and is due to the vanishing of the Pomeranchuk contribution at this point. The K-matrix model predicts the vanishing of the Pomeranchuk term (diffraction zero) to move towards smaller values of $|t|$ in a logarithmic fashion as the energy is increased.

Comparing the set of values I and II we observe (1) that Solution II is closer to exchange degeneracy for P' and ω which has a bearing on the shrinkage pattern as will be discussed below, and (2) that s_0 in Solution II is considerably smaller. Such a small value of s_0 is required in order to obtain a diffraction peak extending over four orders of magnitude. It is well known that changing the value of s_0 to $s_0 < 1$ corresponds to the introduction of residues decaying exponentially with t. The differential cross section is naturally very sensitive to changes in s_0. Total cross sections, on the other hand, are less sensitive to such changes since the residues can always be readjusted in certain limits without altering the goodness of the fit to both total and differential cross sections.

We have examined the interference between the Pomeranchuk term and the absorptive corrected P' and ω contributions, behaving like $1/\sqrt{s}$, in order to determine the energy dependence of the diffraction cone in pp and $p\bar{p}$ scattering, i.e., the shrinkage or antishrinkage at the present energies. It turns out that the following situation is realized in this model. For $(d\sigma/dt)_{pp}$ the ω contribution subtracts from the Pomeranchuk term for $|t|$ smaller than the crossover point ($t_{co} \approx -0.20$ GeV^2) and adds for $|t|$ bigger than the crossover point. The reverse is true for the P' contribution. In a completely exchange degenerate situation the P' and ω contributions cancel and the energy behavior of the pp forward differential cross section shows as a result logarithmic shrinkage due to the Pomeranchuk term alone. The same is true if P'-ω exchange degeneracy in the residues and trajectories is only

slightly broken as in our Solution II. For $p\bar{p}$ scattering, however, both Regge pole contributions of order $1/\sqrt{s}$ add below the crossover point and subtract beyond it, which makes the diffraction peak on the one hand steeper in $p\bar{p}$ compared to pp and on the other hand expanding due to the decaying of the contributions of order $1/\sqrt{s}$ in going to higher energies. Finally, however, at sufficiently high energies also the $p\bar{p}$ differential cross section will show shrinkage according to $\alpha'_{P,\mathrm{eff}}=\alpha'/2$ as the pp diffraction peak does. The structure in $(d\sigma/dt)_{p\bar{p}}$ around $t=-0.8$ GeV^2 — being an effect of the lower lying trajectories — is predicted to disappear with increasing s, whereas the shoulder in $(d\sigma/dt)_{pp}$ at $t=-1.2$ GeV^2 is connected to the Pomeranchuk contribution and will in this model develop into a more profound diffraction minimum with growing energy. We point out, however, that the curves labelled P in Figs. 2 and 3 do not represent asymptotic curves for the differential cross sections at large s but possess themselves a logarithmic energy dependence. This is implied by the statement that diffraction peaks shrink indefinitely in this model as s increases.

We thank Professor S. D. Drell for his kind hospitality at SLAC and Drs. E. Kluge and W. A. Ross for their advice and assistance in using the program MINFUN.

REFERENCES

1. W. Drechsler, Report No. SLAC-PUB-735, Phys. Rev. to be published.
2. R. Blankenbecler and M. L. Goldberger, Phys. Rev. 126, 766 (1962).
3. G. G. Beznogikh et al., Phys. Letters 30B, 274 (1969).
4. S. Frautschi and B. Margolis, Nuovo Cimento 56A, 1155 (1968);
   C. B. Chiu and J. Finkelstein, Nuovo Cimento 57A, 649 (1968).

5. The reason for this is the fact that the pn charge exchange reaction, which is expected to be dominated by isovector exchange, has a very small cross section at high energies. Moreover, these trajectories couple to the spin flip amplitudes which we consistently neglect in this analysis.

6. The connection between τ and D, introduced in reference 1, is $\tau = D/8\pi^2\alpha'^2 s_0^3$.

7. W. Galbraith et al., Phys. Rev. 138, B913 (1965); K. J. Foley et al., Phys. Rev. Letters 19, 857 (1967);
IHEP-CERN Collaboration, Phys. Letters 30B, 500 (1969).

8. V. Barger and R. J. N. Phillips, Phys. Rev. Letters 24, 291 (1970).

9. Remember that terms of order $(\tau/\sigma_{tot}(\infty))^2$ were neglected throughout.

10. K. J. Foley et al., Phys. Rev. Letters 15, 45 (1965); J. Orear et al., Phys. Rev. 152, 1162 (1966); K. J. Foley et al., Phys. Rev. Letters 11, 503 (1963); D. Harting et al., Nuovo Cimento 38, 60 (1965).

11. D. Birnbaum et al., Phys. Rev. Letters 23, 663 (1969);
J. V. Allaby et al., Phys. Letters 28B, 67 (1968).

12. The dependence of $d\sigma/dt$ on τ comes about through the absorptive correction of the P' and ω contributions.

FIGURE CAPTIONS

1. Fit to (a) total cross sections and (b) ratio of real to imaginary part at t=0 of Ref. 7. I: Solution I [P Pomeranchuk contribution alone]; II: Solution II.

2. Comparison with the pp data of Ref. 11 at p_{lab}=19.2 GeV/c. I: Solution I; II: Solution II [P Pomeranchuk contribution alone].

3. Comparison with the $p\bar{p}$ data of Ref. 11 at p_{lab}=16 GeV/c. I: Solution I; II: Solution II [P Pomeranchuk contribution alone].

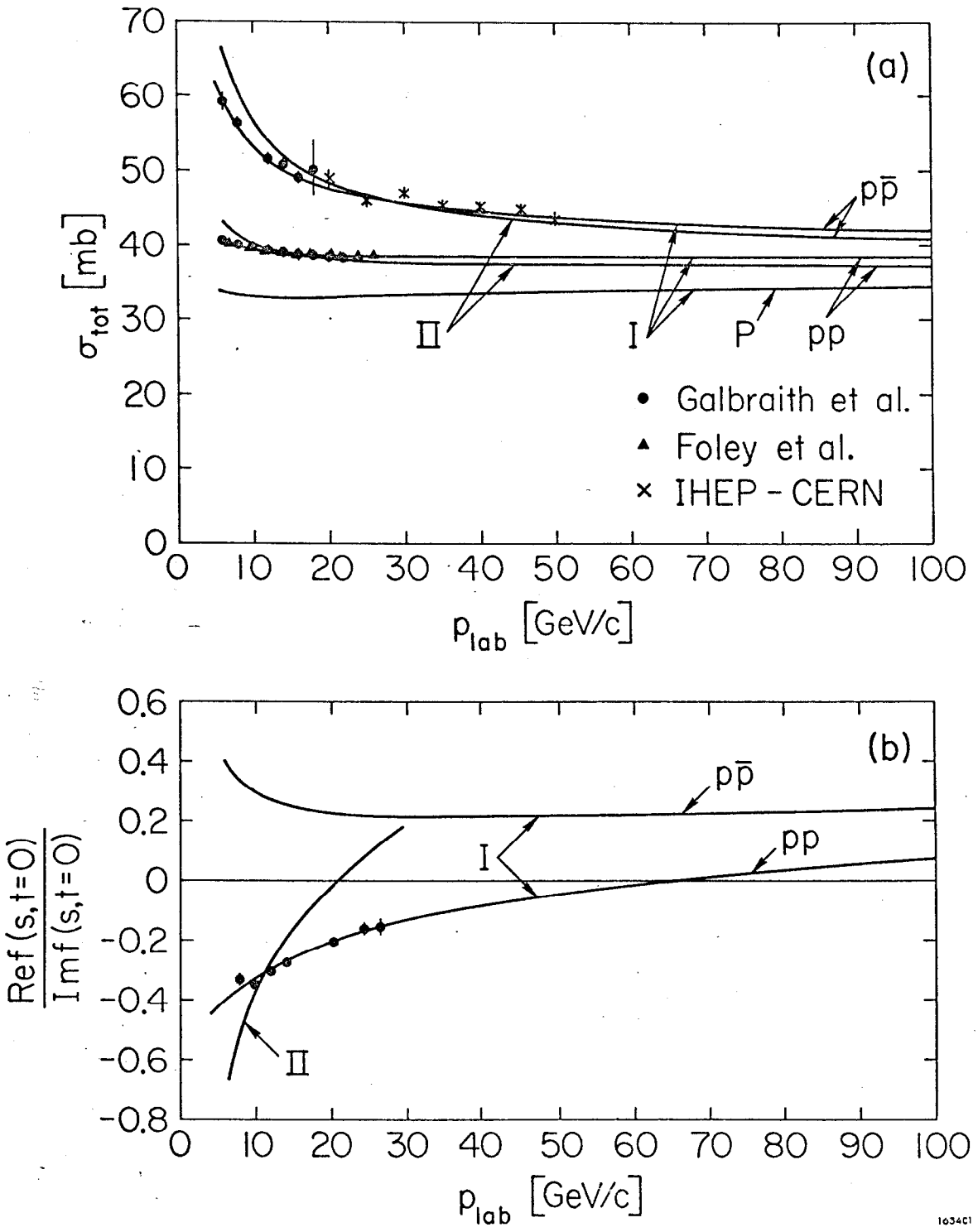
(a)
σ_{tot} [mb]
p_{lab} [GeV/c]
$p\bar{p}$
pp
II
I
P
Galbraith et al.
Foley et al.
IHEP - CERN
(b)
$\frac{Ref(s,t=0)}{Imf(s,t=0)}$
$p\bar{p}$
pp
I
II
p_{lab} [GeV/c]
163401

Fig. 1

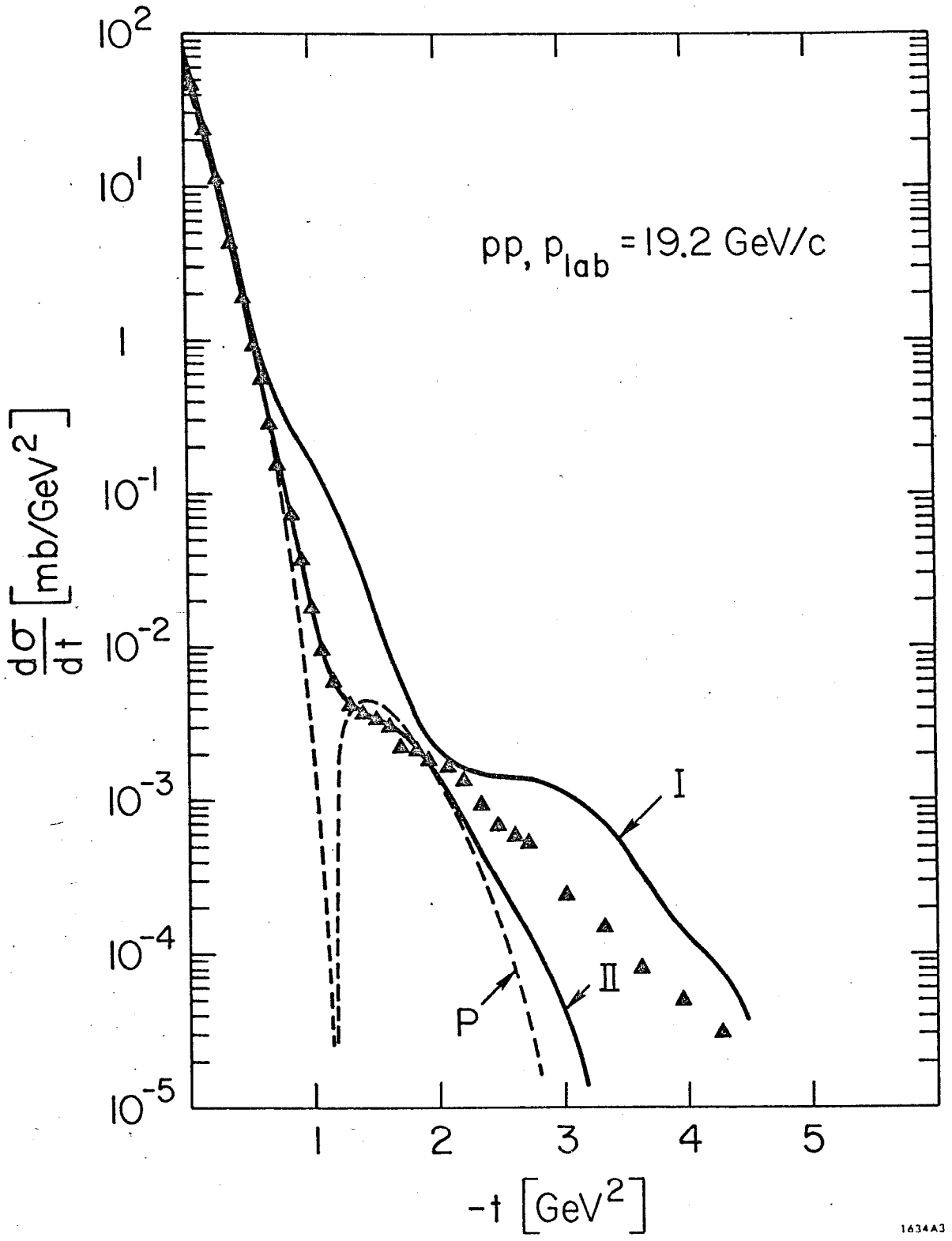
pp, p_{lab} = 19.2 GeV/c
$\frac{d\sigma}{dt}$ [mb/GeV^2]
10^2
10^1
1
10^{-1}
10^{-2}
10^{-3}
10^{-4}
10^{-5}
1
2
3
4
5
-t [GeV^2]
I
II
P
1634A3

Fig. 2

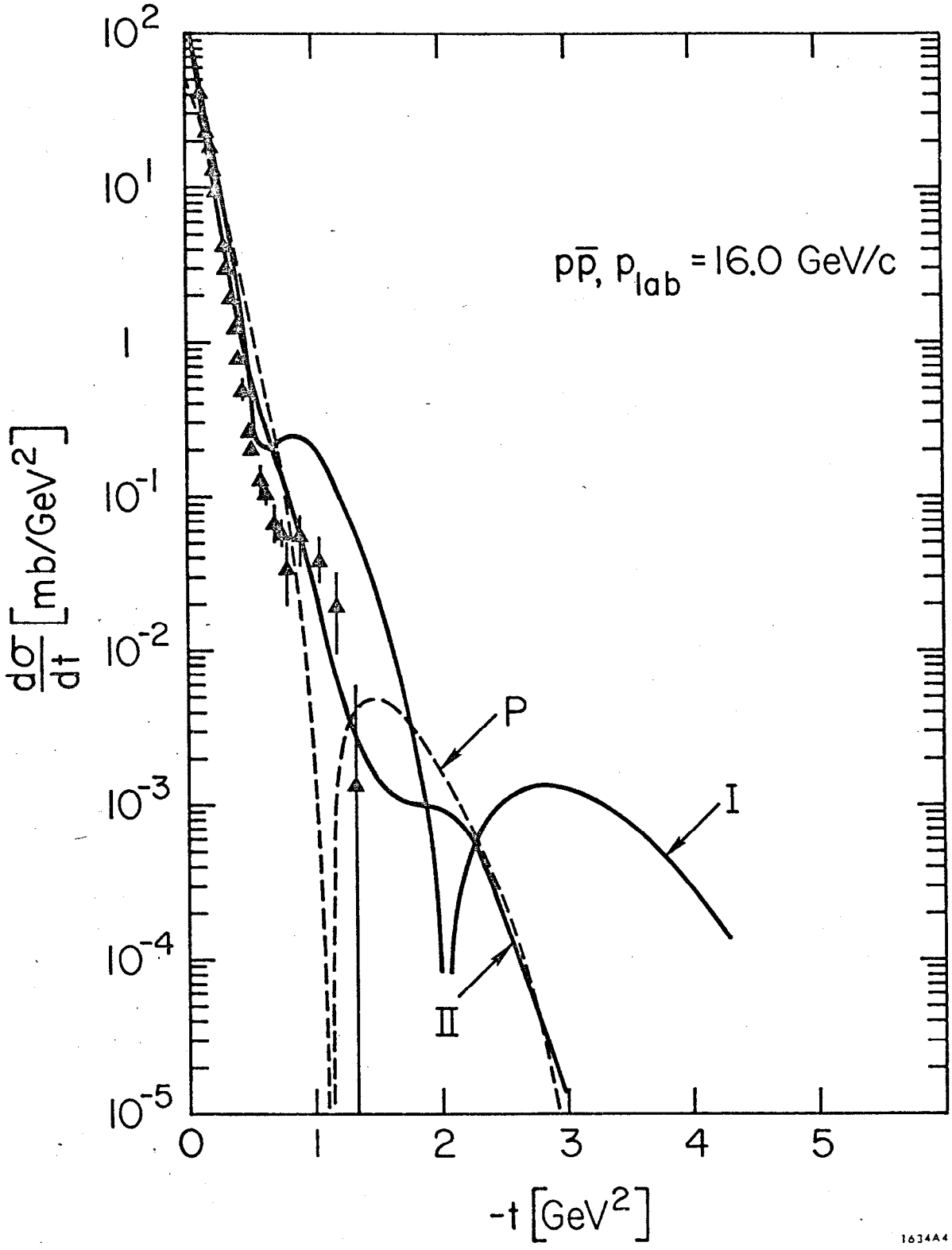
10^2
10^1
1
10^{-1}
10^{-2}
10^{-3}
10^{-4}
10^{-5}
$\frac{d\sigma}{dt}$ [mb/GeV^2]
$p\bar{p}$, p_{lab} = 16.0 GeV/c
P
I
II
0
1
2
3
4
5
-t [GeV^2]
1634A4

Fig. 3